Available online at www.sciencedirect.com

ScienceDirect

Polymer 48 (2007) 6384–6394

polymer

www.elsevier.com/locate/polymer

Reducing electrospun nanofiber diameter and variability using cationic amphiphiles

Kenneth Lin [a], Kian-Ngiap Chua [b], Gregory T. Christopherson [a], Shawn Lim [c], Hai-Quan Mao [a,*]

[a] *Department of Materials Science and Engineering, Johns Hopkins University, Baltimore, MD 21218, USA*
[b] *Division of Bioengineering, and Nanoscience and Nanotechnology Initiative, National University of Singapore, Singapore*
[c] *Department of Biomedical Engineering, Johns Hopkins University School of Medicine, Baltimore, MD 21205, USA*

Received 23 May 2007; received in revised form 17 August 2007; accepted 22 August 2007
Available online 28 August 2007

Abstract

One major limitation of the electrospinning technique for generating polymer fibers is the large average diameter and the broad diameter variability of electrospun fibers. Improved methods of controlling fiber diameter and variability will have implications for many applications ranging from filtration to cell and tissue engineering. Here we report an effective method of reducing the diameter and variability of fibers prepared from three different polymers, poly(ethersulfone), poly(caprolactone), and poly(caprolactone-*co*-ethyl ethylene phosphoester), by doping polymer solutions with a positively charged amphiphile, octadecyl rhodamine (R18) or octadecyltrimethylammonium bromide (OTAB) at 5000:1 to 20:1 of polymer to amphiphile weight ratio. This is due to the combined effect of field-driven surface partitioning of positively charged amphiphiles and surface tension reduction. This method of diameter reduction can be applied easily without modifying the electrospinning setup or changing the polymer–solvent system.

Keywords: Electrospinning; Polymer fiber; Diameter reduction

1. Introduction

Electrospinning is garnering renewed interest because of its ability to create polymer and ceramic fibers with diameters ranging from tens to hundreds of nanometers [1–3]. The small diameter and high surface area to volume ratio of electrospun nanofibers make them an attractive platform for various biomedical applications, for example, as filtration devices [1], wound healing bandages [4], controlled drug release carriers [5], and cell/tissue engineering scaffolds [6–12].

In a typical setup, non-woven or aligned fibrous matrices of ultra-fine fibers are spun from a viscous solution of a polymer or ceramic precursor subjected to an electric potential, typically between 6 and 30 kV, under which charge accumulates on the surface and to a lesser extent in the bulk of the solution [2,3]. When the Coulombic repulsion force from the accumulated charge on the surface overcomes the surface tension and the viscoelastic force of the solution, a charged jet ejects towards a collector plate of opposite polarity. As the jet travels to the plate, it thins down due to stretching and bending instabilities and then deposits randomly as a nanofiber mesh [1–3] or on a rotating wheel as an aligned fiber bundle [6,13]. Despite numerous studies on electrospinning of various polymers, control over the characteristics of the fibers (fiber diameter, morphology, pore size of the fiber mesh, etc.) remains empirical by adjusting the typical spinning parameters such as flow rate, applied voltage, collecting distance between needle and ground electrode, and polymer solution properties such as solvent, concentration, conductivity, and surface tension [14–16]. As a result, electrospun polymer fibers usually exhibit a wide range of fiber diameters in a typical preparation.

---

* Corresponding author. Department of Materials Science and Engineering, Johns Hopkins University, 102 Maryland Hall, 3400 N. Charles Street, Baltimore, MD 21218, USA. Tel.: +1 410 516 8792; fax: +1 410 516 5293.
E-mail address: hmao@jhu.edu (H.-Q. Mao).

0032-3861/$ - see front matter © 2007 Elsevier Ltd. All rights reserved.
doi:10.1016/j.polymer.2007.08.056

This variability poses a significant problem in applications where the performance of nanofiber meshes is influenced by fiber diameter. For instance, a filtration nanofiber membrane will have better diffusion, interception, and inertial impaction efficiencies with a more uniform and smaller fiber diameter [1]. An artificial cornea will require the use of a scaffold transparent to visible light, this requires the fiber diameter to be significantly smaller than wavelengths of visible light [17]. When nanofibers are used as artificial extracellular matrices for cell and tissue engineering, fiber diameter has been shown to significantly influence many cellular processes of osteoprogenitors [18], vascular endothelial cells [19] and fibroblasts [20] that are cultured on the fiber meshes. It is widely hypothesized that fibers with diameters approaching that of collagen fibrils (30–400 nm) in natural extracellular matrix can offer topographical features favorable to cell response [21]. A methodology that can easily control fiber diameter and distribution is urgently needed to define correlations between fiber diameter and cell adhesion, proliferation and differentiation.

A mathematical model for electrospinning shows fiber diameter to be a function of surface tension, flow rate, and electric current [3]. Fiber diameter increases with surface tension and flow rate, but decreases with electric current. Nanofiber diameter is commonly changed by adjusting the polymer concentration, with lower concentrations resulting in thinner fibers [14]. However, for any given polymer–solvent combination, a threshold concentration exists below which fibers cannot be formed. This threshold hence determines the lower limit for reducing fiber diameter by adjusting polymer concentration. Furthermore, the jet unevenly stretches during whipping as a result of axisymmetric and non-axisymmetric instabilities due to the perturbations of surface charges [22], generating fibers with wide fiber distribution. This is particularly the case for polymer solutions with lower conductivities.

One way to alleviate this problem is to use additives to further tailor the properties of the solution. Charged molecules such as salts can be added to increase the solution conductivity and net charge density of the electrospun polymer jet [23,24]. It has been shown that the average diameter of electrospun fibers decreases as solution conductivity increases, due to the increased stretching force exerted on the charged jet [16]. Cationic surfactants have also been used to prevent bead formation in electrospun fibers [22]. We hypothesized that charged amphiphiles could also be used to reduce fiber diameter by reducing the surface tension of polymer solution. Here we report the incorporation of cationic amphiphiles as a simple method to reduce the diameter and variability of the polymer nanofibers and demonstrate that this method can be applied to several polymer–solvent systems.

2. Experimental

2.1. Materials

Poly(ethersulfone) (PES) with M_w of 55,000 was purchased from Goodfellow Cambridge Limited, UK. Poly(caprolactone) (PCL) with M_w of 65,000 was purchased from Sigma–Aldrich. Poly(caprolactone-*co*-ethyl ethylene phosphoester) (PCLEEP) with M_w of 70,760 was synthesized as described by Wen and Leong [25]. Dimethyl sulfoxide (DMSO) was purchased from J.T. Baker. Octadecyl rhodamine B (R18) was purchased from Invitrogen. Rhodamine B (RhB) and octadecyltrimethylammonium bromide (OTAB) were from Sigma–Aldrich.

2.2. Electrospinning

PES was dissolved in DMSO at varying concentrations ranging from 5 to 25 wt% and loaded in a plastic syringe fitted with a 27 G needle. A syringe pump (KD Scientific, USA) was used to feed the polymer solution into the needle tip at a fixed feed rate of 0.3 mL/h. The PES nanofiber meshes were fabricated by electrospinning at 13–15 kV using a high voltage power supply (Gamma High Voltage Research, USA). Nanofibers were collected onto grounded 15-mm diameter glass coverslips (Paul Marienfeld, Germany) with a needle tip to collector distance of 160 mm. The deposited nanofiber samples were then placed under vacuum to remove residual DMSO, and subsequently dried and stored in a desiccator. To investigate the effect of R18 on fiber diameter, R18 was dissolved in 22 wt% PES solution (with reference to solvent) at a final concentration of 0.03, 0.1, 0.3 and 0.5 wt% with reference to polymer mass in the solution. PES fibers doped with OTAB were electrospun with similar conditions but with a feed rate of 0.5 mL/h. OTAB was first dissolved in a minimal amount of methanol before addition to PES solution for final concentrations of 0.01, 1 and 5 wt% of total PES mass in solution.

PCLEEP fibers were electrospun from PCLEEP copolymer solution in acetone (21.5 wt%) using the same electrospinning apparatus and conditions as described above. For spinning with R18 doping, R18 was dissolved in PCLEEP solution at final concentrations of 0.02, 0.1, 0.5, and 1 wt% with reference to PCLEEP mass in solution.

PCL fibers were electrospun from a 12 wt% PCL solution in a solvent mixture of dichloromethane and methanol at a 4:1 weight ratio. Electrospinning occurred at 1.0 mL/h flow rate and 12 kV. R18 was dissolved in PCL solution at final concentrations of 0.1 and 1 wt% with reference to PCL mass in solution. OTAB was dissolved in PCL solution at final concentrations of 0.1, 1, and 5 wt% with reference to PCL mass in solution.

In order to investigate the radial distribution of charged molecules during the spinning process, Rhodamine B and R18 were incorporated into 12 wt% PCL solution at a concentration of 0.4 wt% with reference to polymer mass in solution. The solutions were electrospun at 2.0 mL/h and 10 kV. The distribution of Rhodamine B and R18 was imaged under a Nikon TE2000 fluorescence microscope (Nikon, USA).

2.3. Characterization of fiber diameters

Electrospun fibers were imaged using a scanning electron microscope (SEM, JEOL 6700F) after gold-sputter coating

(~4 to 6 nm thickness). The average diameter of the fibers was analyzed from the SEM images of the fibers using the National Institutes of Health ImageJ software [26]. High resolution (1280 × 1024 pixels) tif images were used for image analysis. At least 40 different fibers were analyzed for each electrospinning condition. For each fiber analyzed, several diameter measurements were made along the axial length of the fiber and averaged together to find the diameter of one fiber. Results were reported as mean ± standard deviation (variability). Variability was quantified as standard deviation/mean (%). Fiber diameter was plotted with normalized frequency as a way to visually show the variability. Normalized frequency is defined as the ratio of fibers found within a small diameter range (50 nm) to the total number of fibers. Statistical analysis was performed with two-tailed Student's *t*-test. A *p* value of less than 0.05 was considered statistically significant. Curve fitting of fiber diameter variability was performed with SigmaPlot (Systat 2001).

2.4. Characterizations of viscosity, conductivity, surface tension and the release of R18

The viscosities of PES/DMSO solutions at different PES concentrations were measured at 25 °C using an ARES

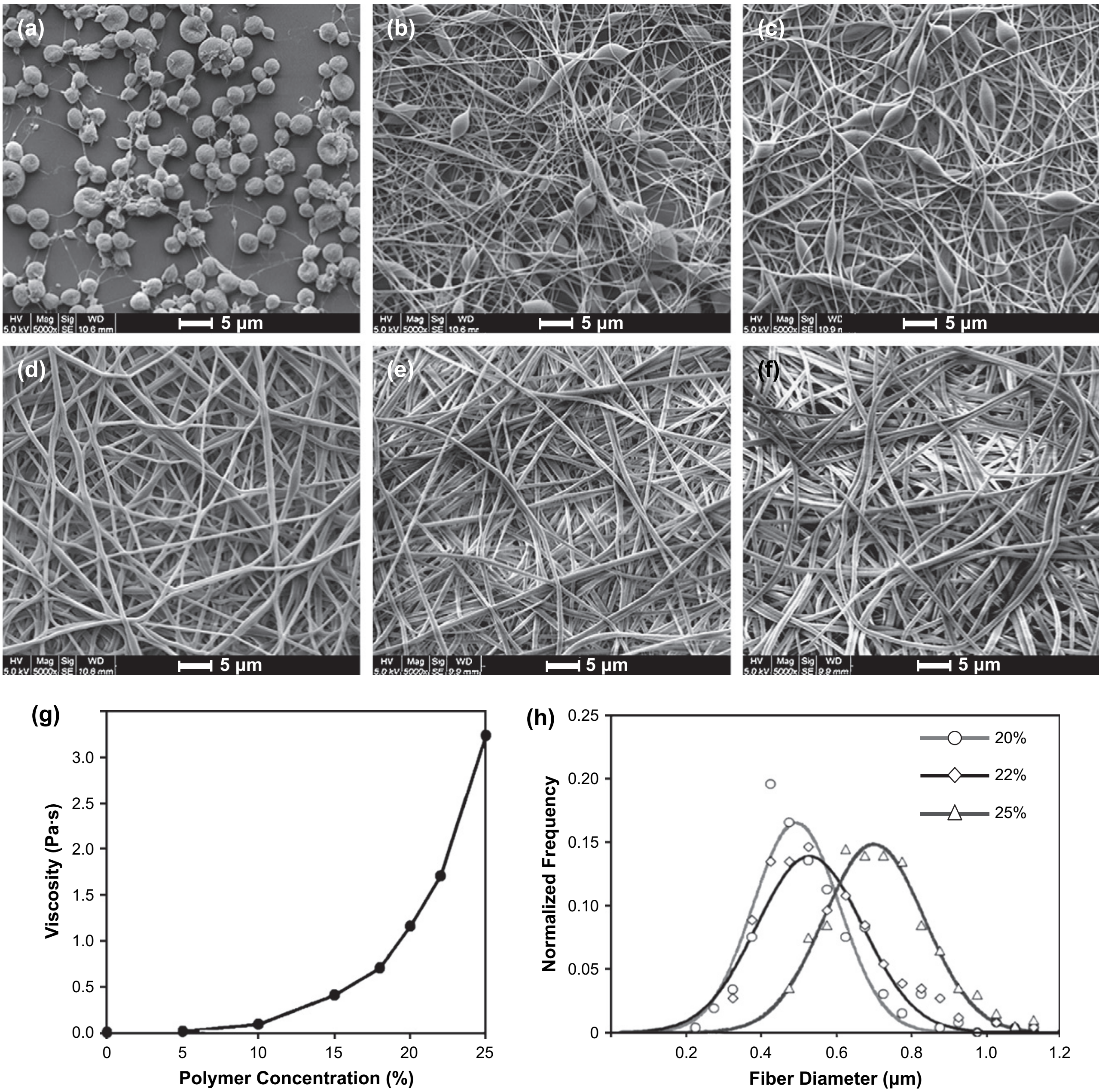

Fig. 1. Scanning electron microscopic images of PES fibers electrospun from PES solutions in dimethyl sulfoxide (DMSO) of different concentrations (flow rate 0.3 mL/h): (a) 5 wt%, (b) 10 wt%, (c) 15 wt%, (d) 20 wt%, (e) 22 wt% and (f) 25 wt%; (g) effect of PES concentration on solution viscosity; (h) diameter distribution of PES fibers as a function of PES solution concentration.

rheometer (TA Instruments, USA) in a Couette geometry with a gap size of 20 μm. Relative conductivity measurements were taken using a Solartron Schlumberger 1255 Frequency Response Analyzer and a 1286 Electrochemical Interface (Solartron, USA). Surface tension measurements were taken using the pendant drop method [27] on a Raméhart Model 200 Goniometer with DROPimage software (Ramé-hart, USA).

Fluorescence measurements of R18 leached from fibers were taken with a Gemini XPS spectrofluorometer at $\lambda_{ex} = 560$ nm and $\lambda_{em} = 585$ nm (Molecular Devices, USA).

2.5. Cell culture on R18-loaded fibers

Mouse NIH3T3 fibroblasts were maintained and cultured in DMEM media supplemented with 10% FBS and placed in

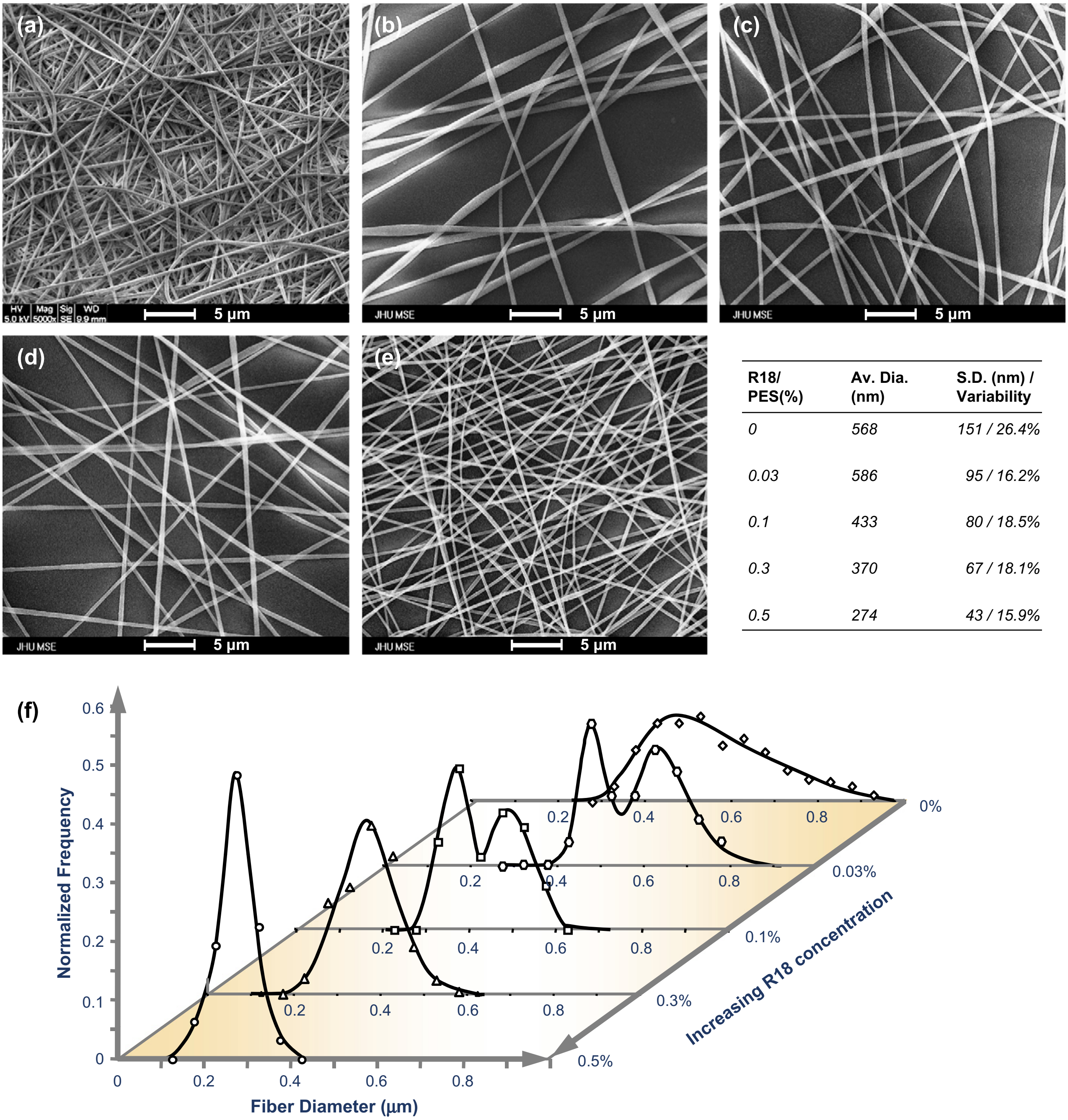

R18/ PES(%)	Av. Dia. (nm)	S.D. (nm) / Variability
0	568	151 / 26.4%
0.03	586	95 / 16.2%
0.1	433	80 / 18.5%
0.3	370	67 / 18.1%
0.5	274	43 / 15.9%

Fig. 2. Effect of R18 incorporation on PES fiber diameter. Scanning electron microscopic images of PES fibers prepared from 22 wt% of PES solution in DMSO containing different concentrations of R18 with reference to PES mass (flow rate: 0.3 mL/h): (a) 0%, (b) 0.03%, (c) 0.1%, (d) 0.3% and (e) 0.5%; (f) diameter distribution of PES fibers as a function of R18 concentration in dry fibers. Differences between means were significant with $p < 0.01$ when R18 to PES ratio was higher than 0.1%.

a 37 °C and 5% CO_2 atmosphere. The cells were seeded at a density of 50,000 cells/cm^2 on PES fiber mesh doped with 0.5 wt% R18 according to a method we reported previously [10,28]. After 24 h, the cells were removed by incubating with 0.05% trypsin/EDTA solution and gentle pipetting. Cells were re-seeded on a tissue culture plate for 30 min at 37 °C in culture medium and imaged under a Nikon fluorescence microscope. Harvested fibers were also imaged under the same settings.

3. Results and discussion

The goal of this study is to investigate the effect of positively charged amphiphiles, either octadecyl rhodamine (R18) or non-fluorescent octadecyltrimethylammonium bromide (OTAB), in polymer solution on the diameter of electrospun fibers. We chose these two molecules because of their good solubility in organic solvent, their surface activity, and their electrostatic charge. These characteristics modify surface tension and electroconductivity of the polymer solution, and therefore modulate the fiber diameter and spinnability of the polymer solution.

In order to test the applicability of such an approach, we have tested the effect of R18 and OTAB on three different polymers: polycaprolactone (PCL), poly(caprolactone-*co*-ethyl ethylene phosphoester) (PCLEEP), and poly(ethersulfone) (PES). PCL and PCLEEP are degradable polymers [10,29]; and electrospun PCL and PCLEEP nanofibers have been used for liver tissue engineering [10] and to promote peripheral nerve regeneration [30]. PES is a non-degradable polymer that has been widely used in hemodialysis, biopharmaceutical and filtration applications because of its good biocompatibility, chemical resistance, and membrane processability [31–33]. PES nanofibers have recently been used as a scaffold for expansion of umbilical cord blood-derived hematopoietic stem cells [10,28].

3.1. PES fibers without R18 supplementation

Solvent choice and polymer concentration are important parameters that influence the quality of electrospun fibers. DMSO was chosen over other possible solvents because of its higher dielectric constant.

The viscosity of PES solution increased exponentially as the polymer concentration increased (Fig. 1g). The minimum concentration required to achieve non-beaded fibers was 20 wt%, which corresponded to a minimum viscosity of

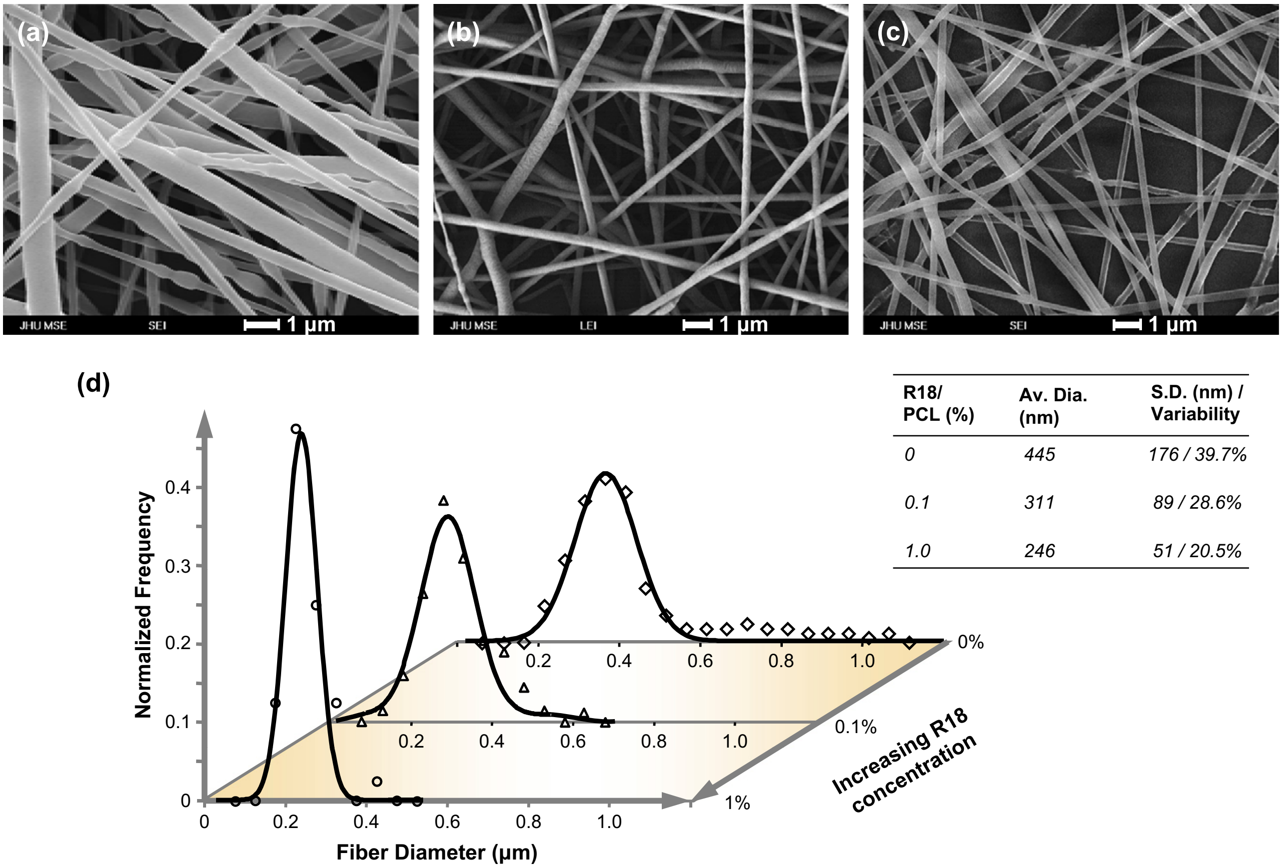

R18/ PCL (%)	Av. Dia. (nm)	S.D. (nm) / Variability
0	*445*	*176 / 39.7%*
0.1	*311*	*89 / 28.6%*
1.0	*246*	*51 / 20.5%*

Fig. 3. Effect of R18 incorporation on PCL fibers. Scanning electron microscopic images of PCL fibers prepared from 12 wt% of PCL solution in dichloromethane/methanol (4:1, v/v) containing different concentrations of R18 with reference to PCL mass (flow rate: 1.0 mL/h): (a) 0%, (b) 0.1%, (c) 1%; (d) diameter distribution of PCL fibers as a function of R18 concentration in dry fibers. Differences between means were significant with $p < 0.01$.

1155.7 mPa s. PES solutions with lower concentration or viscosity yielded electrospraying of beads (5–10 wt% with viscosities of 14.1–86.7 mPa s) or highly beaded fibers (15–18 wt% with viscosities ranged from 408.1 to 705.0 mPa s) as seen in Fig. 1a–c.

Fig. 1h shows the normalized frequency distribution of the fiber diameters for different polymer concentrations. The average fiber diameters for 20, 22, and 25 wt% PES solutions (Fig. 1d–f) ranged from 529 ± 144, 568 ± 151, and 719 ± 144 nm, respectively. This observation is consistent with the literature on the effect of concentration [15]. At low concentration, incomplete drying of the residual solvent from the solution jet resulted in bead formation on the wet fiber due to surface tension. At high concentration, the high viscosity of PES solution limited the extent of jet stretching during whipping. At intermediate concentrations, beaded fibers were obtained due to the charge instability and surface tension effect. The lowest average fiber diameter was about 530 nm (Fig. 1d). Furthermore, the diameter range of PES nanofibers collected under these conditions was relatively wide, typical of E-spun polymer nanofibers.

3.2. Fiber diameter reduction by incorporation of R18 in polymer solutions

Incorporation of R18 into PES solution significantly reduced fiber diameter and its size variability with an effective doping level ranging from 0.01 to 0.5 wt% with reference to

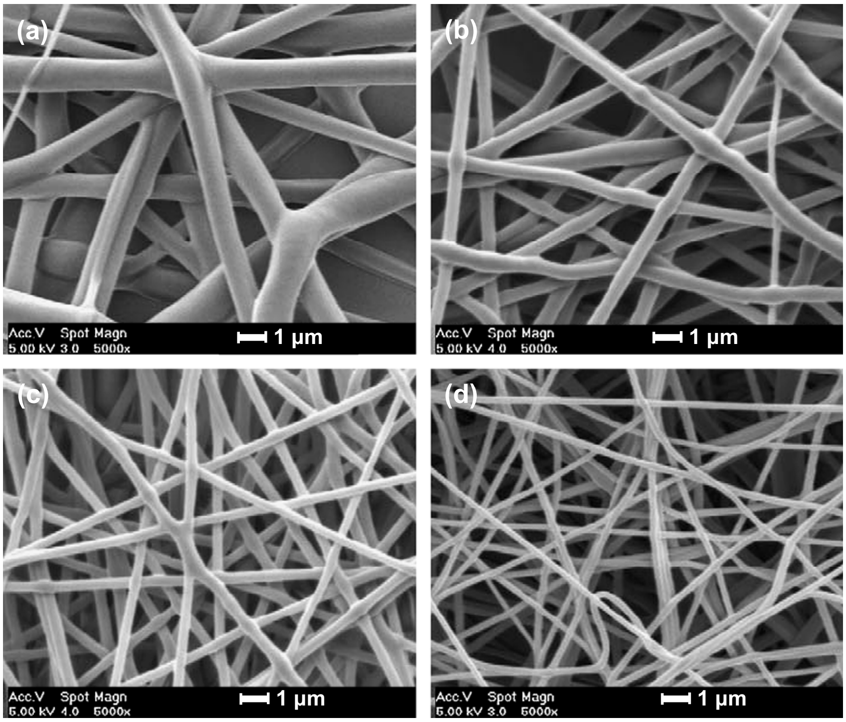

R18/ PCLEEP (%)	Av. Dia. (nm)	S.D. (nm) / Variability
0	790	397 / 50.3%
0.02	466	101 / 21.6%
0.1	336	44 / 13.1%
0.5	263	47 / 17.7%
1.0	201	34 / 16.7%

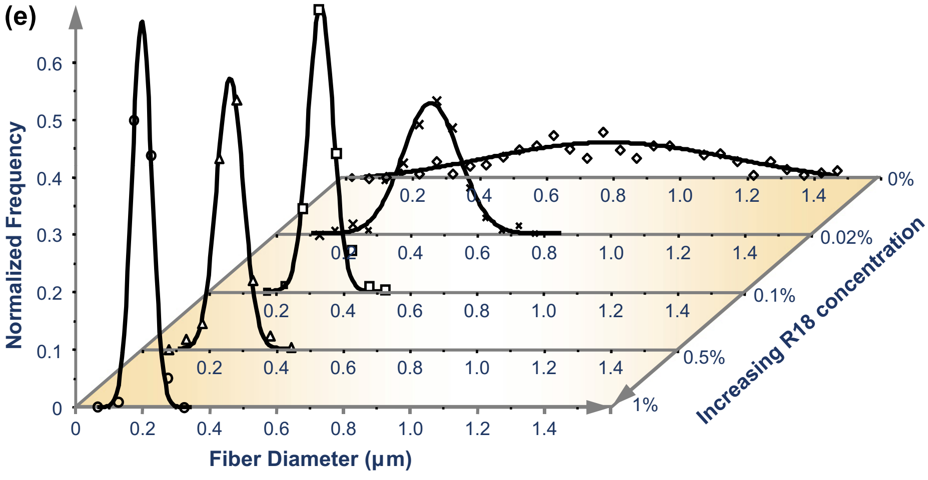

Fig. 4. Effect of R18 incorporation on PCLEEP fiber diameter. Scanning electron microscopic images of PCLEEP fibers prepared from 21.5 wt% of PCLEEP solution in acetone containing different concentrations of R18 with reference to PCLEEP mass (flow rate: 0.3 mL/h): (a) 0%, (b) 0.02% (c) 0.1%, (d) 1%; (e) diameter distribution of PCLEEP fibers as a function of R18 concentration in dry fibers. Differences between means were significant with $p < 0.05$.

polymer mass in solution. Fig. 2 shows that as R18 concentration increases, PES fiber diameter and variability decrease significantly ($p < 0.01$ for a R18 to PES ratio of higher than 0.1%). With 0.5 wt% R18 doping level (equivalent to 200:1 of PES to R18 weight ratio), PES fiber diameter was reduced to 274 ± 43 nm (15.9% variability) from an undoped diameter of 568 ± 151 nm (26.4%). With 0.03–0.1 wt% R18 doping level (3333:1 to 1000:1 of PES to R18 weight ratio), PES fibers exhibited a minor degree of bead formation. This led to a bimodal distribution of the resulting fiber diameters.

We anticipated that this method could also be applied to electrospinning of other polymers. To demonstrate this, R18 was added to PCL and PCLEEP solutions and it showed similar effect on PCL and PCLEEP fibers—decreased fiber diameter and variability. PCL fibers decreased in size and variability as R18 concentration increased from an undoped fiber diameter of 445 ± 176 nm (39.7%) to 246 ± 51 nm (20.5%) with 1 wt% R18 with reference to polymer mass (Fig. 3). PCLEEP fibers showed the most dramatic decrease in diameter with an undoped fiber diameter of 790 ± 397 nm (50.3%) to 201 ± 34 nm (16.7%) with 1 wt% R18 (Fig. 4). These two polymer solutions exhibited greater sensitivity to the addition of R18, with substantially reduced fiber diameter observed at a R18 concentration of just 0.1 wt% of the overall polymer mass in solution.

3.3. Removal of R18 from the fiber

The presence of R18 in the electrospun fibers may not be ideal for some applications. For example, in cell biology studies, R18 fluorescence in the fibers could interfere with cellular immunofluorescence staining, particularly when R18 doping level is high. In addition, R18 could leach out of the fibers, and may transfer to cells that are cultured on the fibers. However, this release is dependent on the diffusion rate of amphiphiles in polymer fiber and its solubility in aqueous medium. R18 in PES fibers was not significantly released (2%) after soaking in 100% ethanol at room temperature over 6 h with 5 solvent-changes (Fig. 5a). The release in aqueous media is expected to be less pronounced. To test the potential transfer of R18 to cells, we cultured NIH3T3 fibroblasts on R18-loaded PES fibers for 24 h, after which cells were trypsinized and re-seeded on a tissue culture plate for 30 min in order to image any transferred amount of R18 to fibroblasts (direct imaging before separating cells from fibers proved difficult due to the spreading of cells on fibers). Under the fluorescent microscope, we did not observe any significant level of fluorescence either in or on the cells (Fig. 5c), in sharp contrast to the high level of R18 fluorescence in the harvested fibers under the same settings (Fig. 5b). The release of R18 understandably is dependent on the diffusion of the amphiphile in fiber materials. For example, nearly all R18 (98.3%) in PCL fibers was leached out with ethanol washes over 6 h (Fig. 5a). This is likely due to the higher diffusion coefficient of R18 in PCL matrix [11]. For PCL fibers used in cell culture studies, we typically remove all R18 through repeated ethanol washes; and R18 residue in PES fibers did not seem to affect the culture of adult rat neural stem cells [12].

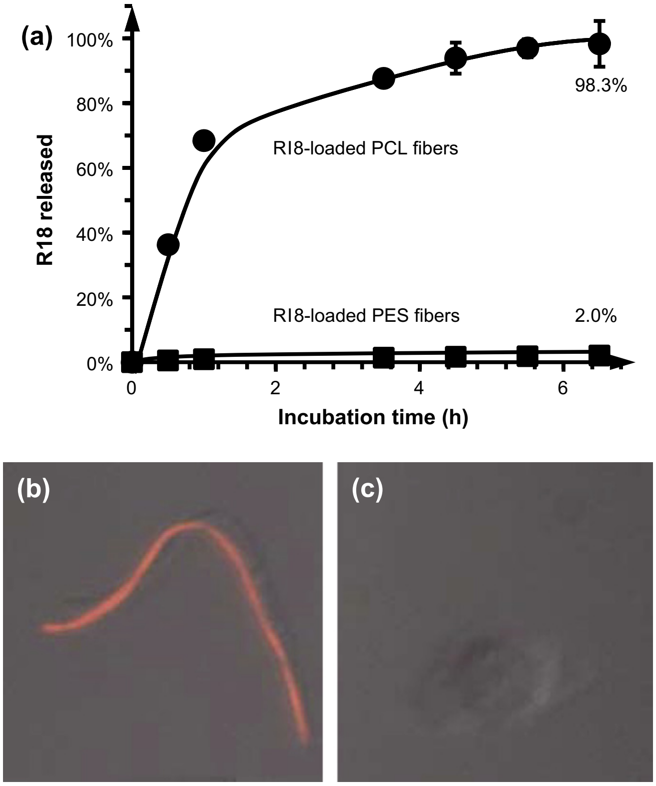

Fig. 5. Removal of R18 from fibers: (a) percentage of R18 removed over time from PCL fiber mesh with 0.1 wt% R18 and PES fiber mesh with 0.5 wt% R18 by multiple ethanol washing. Washing solutions were changed at each marked time point; (b,c) merged fluorescence and phase contrast images show a recovered fluorescing fiber following cell culture in (b) and a non-fluorescent NIH3T3 cell after re-seeding in (c).

3.4. Fiber diameter reduction in electrospinning of OTAB containing polymer solutions

The difficulties posed by the high fluorescence of R18 can be sidestepped by replacing R18 with OTAB, a non-fluorescent and cationic amphiphile. It showed a similar effect to R18 on nanofiber diameter and variability for both PES (Fig. 6) and PCL (Fig. 7). Higher OTAB doping reduced the average diameter and the variability. PES fiber diameters were reduced to 330 ± 59 nm (17.9%) with 5 wt% OTAB from an undoped diameter of 1145 ± 164 nm (14.3%) when electrospun with a flow rate of 0.5 mL/h (Fig. 6). The smallest diameter obtained for PCL fibers was 279 ± 63 nm (22.4%) at 1 wt% OTAB with a flow rate of 0.5 mL/h (Fig. 7). Interestingly, PCL fibers electrospun with a 5 wt% OTAB loading level had a slightly larger average diameter and slightly wider variability than those spun from a solution with 1 wt% OTAB loading. This increase in diameter may be related to the appearance of spherical beads along fiber surfaces roughly 100 nm across. These spherical beads were likely formed as a result of phase separation as OTAB oversaturated the PCL solution. Further increase of OTAB concentration beyond

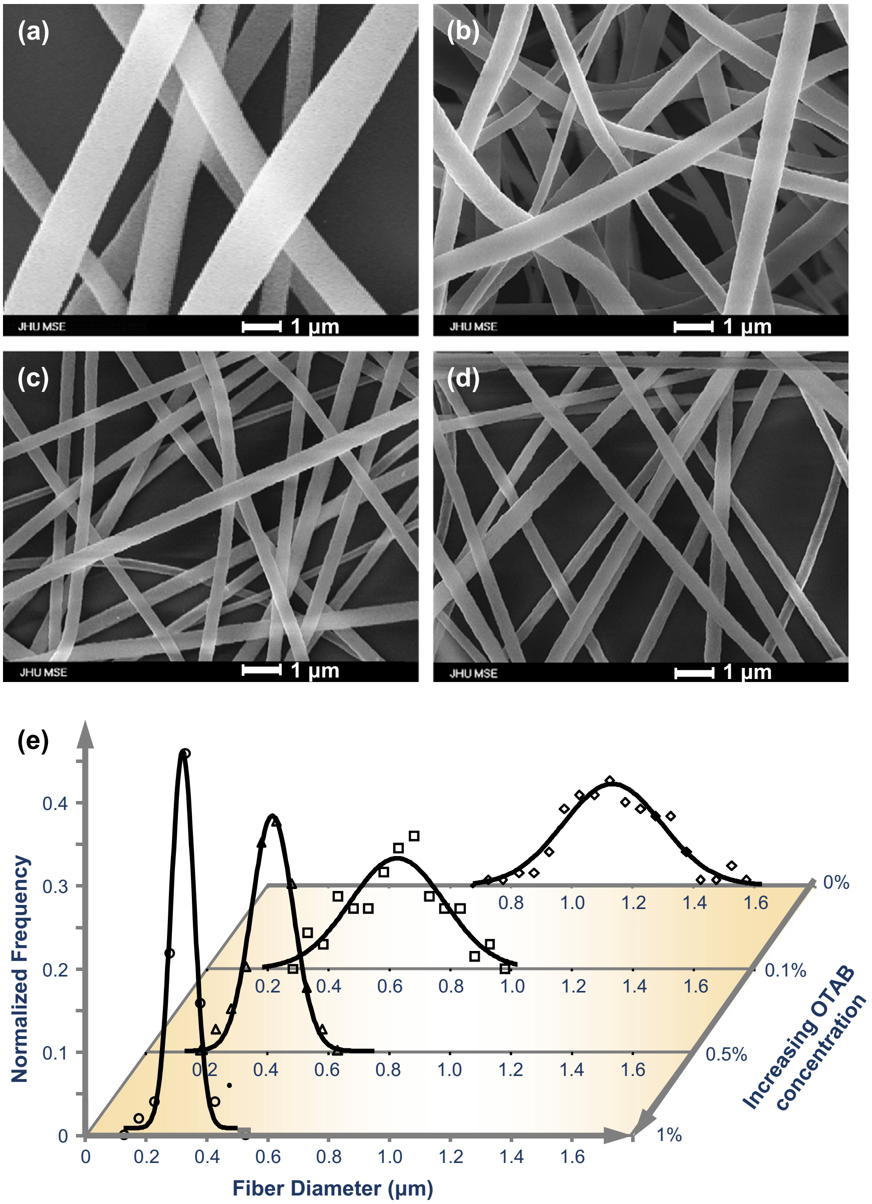

OTAB / PES (%)	Av. Dia. (nm)	S.D. (nm) / Variability
0	*1145*	*164 / 14.3%*
0.1	*618*	*149 / 24.2%*
0.5	*412*	*76 / 18.5%*
1.0	*330*	*59 / 17.9%*

Fig. 6. Effect of OTAB incorporation on PES fiber diameter. Scanning electron microscopic images of PES fibers prepared from 22 wt% of PES solution in DMSO containing different concentrations of OTAB with reference to PES mass (flow rate: 0.5 mL/h): (a) 0%, (b) 0.1%, (c) 0.5%, (d) 5%; (e) diameter distribution of PES fibers as a function of OTAB concentration. Differences between means were significant with $p < 0.01$.

this saturation point had little or no effect on further decreasing of fiber diameter (data not shown). The effect of OTAB on PCLEEP fibers was not tested although comparable results are expected. It is worth noting that, despite the general trend of reducing fiber diameter and variability in the presence of amphiphiles, the effective doping concentrations of the amphiphile should be tested for each polymer–solvent system.

3.5. Mechanism of reduction of diameter and variability by amphiphile doping

The observed reduction of fiber diameter and variability resulted from modification of solution properties by the doped amphiphiles, including solution conductivity, surface tension, solution viscosity, solvent evaporation rate, etc. From literature report, we recognize that the effect on solution viscosity by such a low concentration of amphiphiles (effective concentration was mostly less than 0.22 wt% in the solution) is negligible [22]. We then focused on testing the effect of amphiphile doping on solution conductivity and surface tension, the two major factors affecting electrospinning, by comparing the properties of 12 wt% PCL doped with R18 or Rhodamine B (RhB), a non-amphiphilic analog of R18. RhB and R18 share a similar multi-ring backbone structure and one positively charged amino group, except that RhB lacks the long alkyl chain and hence the amphiphilic characteristic.

Inclusion of R18 and RhB both significantly increased the conductivity of PCL solution, consistent with the literature

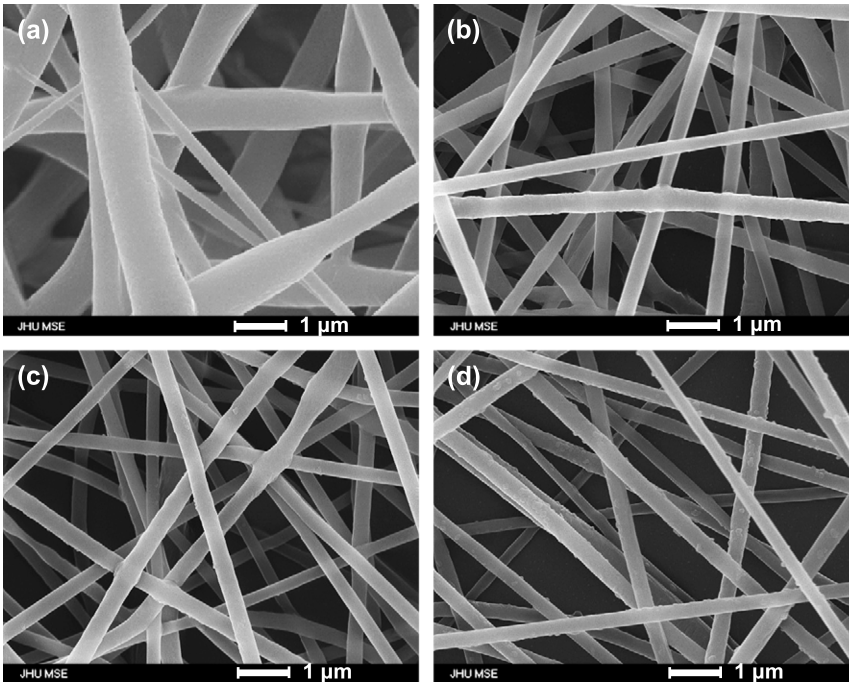

OTAB/ PCL (%)	Av. Dia. (nm)	S.D. (nm) / Variability
0	*445*	*176 / 39.7%*
0.1	*322*	*85 / 26.5%*
1.0	*279*	*63 / 22.4%*
5.0	*326*	*79 / 24.5%*

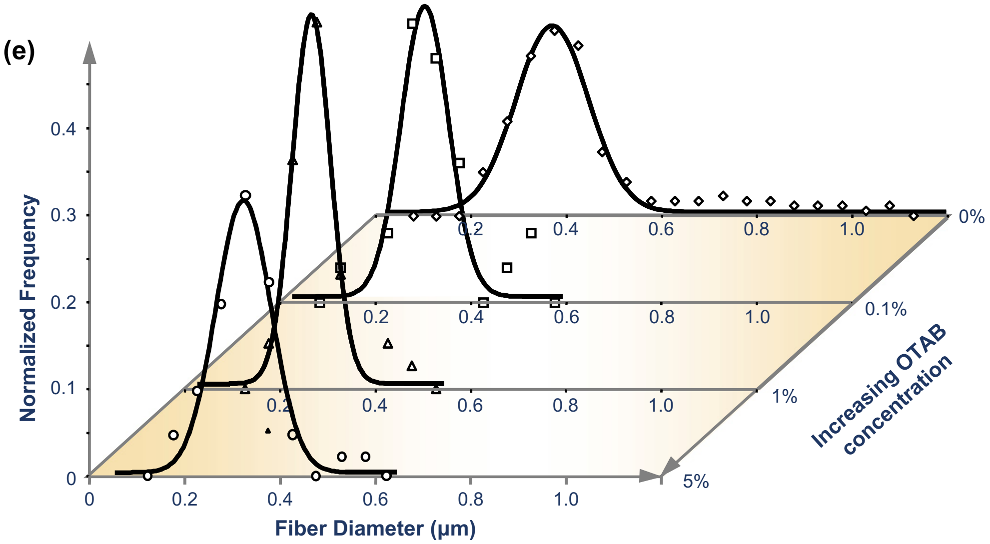

Fig. 7. Effect of OTAB incorporation on PCL fiber diameter. Scanning electron microscopic images of PCL fibers prepared from 12 wt% of PCL solution in dichloromethane/methanol (4:1, v/v) containing different concentrations of OTAB with reference to PCL mass (flow rate: 1.0 mL/h): (a) 0%, (b) 0.1%, (c) 1%, (d) 5%; (e) diameter distribution of PCL fibers as a function of OTAB concentration. Differences between means were significant with $p < 0.05$.

report on effect of charged molecules on solution conductivity [22]. At a 100:1 of PCL to amphiphile weight ratio (the amphiphile concentration in solution was 0.12 wt%), RhB increased conductivity by 4.58 ± 0.03-fold, compared with a 1.90 ± 0.05-fold increase for R18 doping. Based on the theoretical analysis [3], the RhB-loaded polymer jet with higher conductivity, combined with the effect of higher charge repulsion on jet surface due to higher concentration of charges, should enhance jet stretching during whipping more than the R18-loaded jet, therefore yielding smaller diameter fibers. However, doping of RhB in PCL solution at 0.1–5 wt% with reference to PCL mass did not show any noticeable effect on fiber diameter (data not shown).

Surface tension measurement by the pendant drop method showed that, at 100 to 1 ratio of PCL to amphiphile (1 wt% doping concentration with respect to PCL mass), R18 reduced the solution surface tension by 9.7%. In contrast, no significant change was observed for RhB-doped solution under the same condition (Fig. 8a). Lin et al. showed similarly that the surface tension was reduced by a few percent at 0.3 wt% of dodecyltrimethylammonium bromide, a molecule structurally similar to OTAB [22]. Furthermore, under an applied electric field, the positively charged molecule (R18 or RhB) can migrate to the surface of the whipping jet due to the field-driven partition effect, also observed by Sun et al. for charged peptides added to polymer solution [34]. This results in an anisotropic

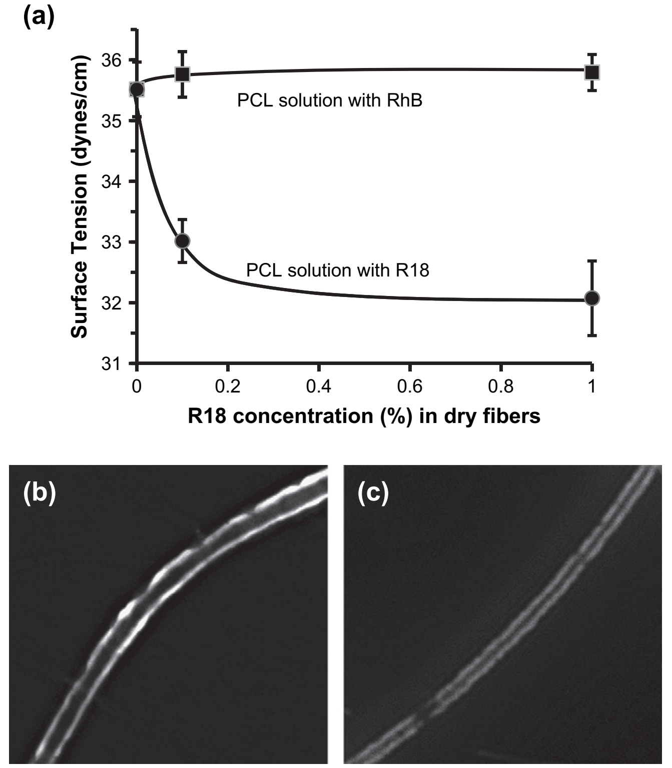

Fig. 8. Mechanism of reduction of diameter and variability by amphiphile doping. (a) Surface tension measurements of 12 wt% PCL solution in dichloromethane/methanol (4:1, v/v) containing R18 or RhB. (b) and (c) Fluorescence images of a R18-doped PCL fiber (b) and a Rhodamine B-doped PCL fiber (c) prepared under same conditions (2 mL/h flow rate, 0.4% doping concentration of R18 and Rhodamine B), showing that R18 and Rhodamine B are primarily located at the periphery of PCL fibers.

distribution of charged molecules in the spinning jet with a higher concentration of the cationic amphiphile on the jet surface. This field-driven partition effect was confirmed by fluorescence microscopic images of the electrospun fibers prepared from both R18 and RhB-doped PCL solutions (Fig. 8b and c), showing that both R18 and RhB were located primarily along the periphery of the doped fibers. These results imply that the impact of amphiphiles on surface tension reduction can be more dramatic (direct surface tension measurement under electrospinning condition was not successful). With a lower surface tension, the whipping jet is more easily elongated by the electrostatic forces, resulting in smaller fiber diameters. Additionally, fibers are more regular due to a more stable jet that encounters fewer perturbations from the surface tension effect of reducing surface area. These analyses are consistent with our data.

Taken together, our results showed that positive charge accumulation on the surface of polymer jet with R18 or RhB in the concentration range tested here was not sufficient to lead to further stretching and thinning of the fiber jet. The surface tension reduction by cationic amphiphiles is likely the primary factor that contributed to the reduction of fiber diameter and variability. In addition, other factors might also play a role in reducing the fiber diameter by amphiphile doping. For example, surface partition of amphiphile may reduce the solvent evaporation rate, thus extending jet stretching and reducing the fiber diameter. Further experiments are needed to reveal a comprehensive mechanism. When extending this conclusion to other charged amphiphiles, it is also important to note that the type of charge on the amphiphile (positive charge in this case) should match the polarity of the electric field applied.

In summary, we report here a simple method of reducing fiber diameter and variability through the addition of positively charged amphiphiles, R18 or OTAB. This manipulation appears to be effective in several different polymer fiber systems. Compared to other methods, this method of diameter reduction can be applied easily without modification of the electrospinning setup or changes to the polymer–solvent system.

Acknowledgements

This work is partially supported by Whiting School of Engineering at Johns Hopkins University through a new faculty startup grant, and a graduate student scholarship to Gregory T. Christopherson from the ARCS Foundation. We would like to thank Prof. James Harden and Prof. Peter Searson for helpful discussion, and Janice Lin for assistance with conductivity measurements.

References

[1] Grafe TH, Graham KM. Fifth international conference on nonwovens filtration; 2003.
[2] Li D, Xia YN. Adv Mater 2004;16:1151–70.
[3] Fridrikh SV, Yu JH, Brenner MP, Rutledge GC. Phys Rev Lett 2003;90:144502.
[4] Khil MS, Cha DI, Kim HY, Kim IS, Bhattarai N. J Biomed Mater Res Part B Appl Biomater 2003;67:675–9.
[5] Kim K, Luu YK, Chang C, Fang DF, Hsiao BS, Chu B, et al. J Controlled Release 2004;98:47–56.
[6] Venugopal J, Ramakrishna S. Appl Biochem Biotechnol 2005;125:147–58.
[7] Pham QP, Sharma U, Mikos AG. Tissue Eng 2006;12:1197–211.
[8] Boudriot U, Dersch R, Greiner A, Wendorff JH. Artif Organs 2006;30:785–92.
[9] Chua KN, Lim WS, Zhang P, Lu H, Wen J, Ramakrishna S, et al. Biomaterials 2005;26:2537–47.
[10] Chua KN, Chai C, Lee PC, Tang YN, Ramakrishna S, Leong KW, et al. Biomaterials 2006;27:6043–51.
[11] Lim S, Liu XY, Song HJ, Mao HQ. Proceedings of the 2006 Materials Research Society Fall Meeting, Boston, MA; 2006.
[12] Christopherson GC, Song HJ, Mao HQ. Proceedings of the 2006 Materials Research Society Fall Meeting, Boston, MA; 2006.
[13] Theron A, Zussman E, Yarin AL. Nanotechnology 2001;12:384–90.
[14] Deitzel JM, Kleinmeyer J, Harris D, Tan NCB. Polymer 2001;42:261–72.
[15] Fong H, Chun I, Reneker DH. Polymer 1999;40:4585–92.
[16] Zong XH, Kim K, Fang DF, Ran SF, Hsiao BS, Chu B. Polymer 2002;43:4403–12.
[17] Bergshoef MM, Vancso GJ. Adv Mater 1999;11:1362–5.
[18] Badami AS, Kreke MR, Thompson MS, Riffle JS, Goldstein AS. Biomaterials 2006;27:596–606.
[19] Xu CY, Yang F, Wang S, Ramakrishna S. J Biomed Mater Res Part A 2004;71A:154–61.
[20] Chen M, Patra PK, Warner SB, Bhowmick S. Tissue Eng 2007.

[21] Abrams GA, Goodman SL, Nealey PF, Franco M, Murphy CJ. Cell Tissue Res 2000;299:39–46.
[22] Lin T, Wang HX, Wang HM, Wang XG. Nanotechnology 2004;15:1375–81.
[23] Choi JS, Lee SW, Jeong L, Bae SH, Min BC, Youk JH, et al. Int J Biol Macromol 2004;34:249–56.
[24] Mit-Uppatham C, Nithitanakul M, Supaphol P. Macromol Chem Phys 2004;205:2327–38.
[25] Wen J, Leong KW. 29th International symposium on control release bioactive Materials, Seoul, Korea; 2002.
[26] Rasband W. ImageJ software, <http://rsb.info.nih.gov/ij/>; 2006. Accessed 5/2006.
[27] Andreas JM, Hauser EA, Tucker WB. J Phys Chem 1938;42:1001–19.
[28] Chua KN, Chai C, Lee PC, Ramakrishna S, Leong KW, Mao HQ. Exp Hematol 2007;35:771–81.
[29] Williams JM, Adewunmi A, Schek RM, Flanagan CL, Krebsbach PH, Feinberg SE, et al. Biomaterials 2005;26:4817–27.
[30] Chew SY, Wen J, Yim EKF, Leong KW. Biomacromolecules 2005;6:2017–24.
[31] Moce-Llivina L, Jofre J, Muniesa M. J Virol Methods 2003;109:99–101.
[32] Unger RE, Peters K, Huang Q, Funk A, Paul D, Kirkpatrick CJ. Biomaterials 2005;26:3461–9.
[33] Unger RE, Huang Q, Peters K, Protzer D, Paul D, Kirkpatrick CJ. Biomaterials 2005;26:1877–84.
[34] Sun XY, Shankar R, Borner HG, Ghosh TK, Spontak RJ. Adv Mater 2007;19:87–91.